Comparison of the analytical and numerical solution of the one-dimensional heat diffusion equation in a transient state applied to a wall

Comparación de la solución analítica y numérica de la ecuación de difusión de calor unidimensional en estado transitorio aplicado a un muro

RUIZ, Francisco†*, HERNANDEZ, Enrique, AGUILAR, Karla and MACIAS, Edgar

ID 1st Author: *Francisco, Ruiz*

ID 1st Coauthor: *Enrique, Hernandez*

ID 2nd Coauthor: *Karla, Aguilar*

ID 3rd Coauthor: *Edgar, Macias*

DOI: 10.35429/JMQM.2020.6.4.22.29 Received March 28, 2020; Accepted June 10, 2020

Abstract

At present the methods of construction have been evolving and one seeks to obtain new materials of construction of housings and buildings looking that are more amicable with the environment and affecting positively the consumer's pocket, knowing that already there exist enough products that are in use for the construction of housings and buildings and knowing that not they all strike favorably to the environment and the economy, we seek to create a product that expires with the requirements of contributing favorably to the environment on having used material that already is a waste and to recycle it to create a sustainable partition that favors the economy of the consumer to the being an insulating product, besides the fact that this partition does not need to be burned in ovens that generate a great pollution. These sustainable partitions are realized by a cellulose mixture in and other amicable materials by the environment and do not damage the ecosystems to the moment to process this product. In this project technology was in use thermography as parameter of thermal efficiency, on tests having fulfilled him and to compare it with other similar products that are in use in the region northwest of the country, giving as result that the insulating sustainable partition I present better results.

Heat Transfer, Thomas Algorithm, Numerical solution

Resumen

La simulación numérica computacional es una herramienta empleada para modelar un fenómeno físico mediante la resolución de las ecuaciones gobernantes con el fin de obtener una solución sin la necesidad de construir un modelo real. En este estudio la transferencia de calor en régimen no estacionario fue simulada analíticamente y posteriormente se comparó con una solución numérica utilizando tres criterios: implícito, explícito y Cranck-Nicholson. La muestra estudiada fue un muro de mampostería común expuesto a 48 horas de transferencia de calor por conducción y convección en una dirección. La transferencia de calor fue resuelta mediante el método de volumen finito. Para tal fin, un código numérico en MATLAB fue desarrollado para discretizar el medio, definir las ecuaciones de equilibrio en cada nodo de la malla y posteriormente resolver las ecuaciones de equilibrio de temperaturas usando una matriz tridiagonal y el Algoritmo de Thomas. El uso de cada esquema de cálculo depende de la magnitud del diferencial de espacio de la malla de estudio y del diferencial de tiempo. Las diferencias promedio en los puntos de interés fueron desde 4% hasta 10% dependiendo del paso de tiempo y espacio.

Transferencia de calor, Algoritmo de Thomas, Solución numérica

Citation: RUIZ, Francisco, HERNANDEZ, Enrique, AGUILAR, Karla and MACIAS, Edgar. Comparison of the analytical and numerical solution of the one-dimensional heat diffusion equation in a transient state applied to a Wall. Journal-Mathematical and Quantitative Methods. 2020. 4-6: 22-29

* Correspondence to Author (email: 152D19004@ujat.mx)
† Researcher contributing first author

Introduction

Building walls are exposed to the three heat transfer mechanisms: conduction, due to the difference in temperatures between the interior and exterior; radiation, due to solar activity; and convection, due to the flow of air masses over the wall surfaces. All these mechanisms can be represented by analytical and numerical models to approximate and evaluate the different variables of the phenomenon. Analytical methods aim to obtain exact solutions from a physical experiment in which the geometry is easily described using a reference system. This method uses the differential equation that describes the problem and its boundary conditions are required to solve the problem. On the other hand, numerical methods are required when the geometry of the system is complex, the boundary conditions are dependent on time, and the properties of the system are a function of temperature. The differences between these two methods are sometimes so small that there are no major implications during the discussion of the results. But it is necessary to make sure that all the variables are represented in the proper way in the equations.

Many comparisons between these two ways of obtaining results have been published, Wang et al, (2014) [1] determined that the largest differences between both methods occur during the beginning of the experiment, but that after a while the models converge to similar solutions.

Also, it was determined that the differences are greater when the values of the properties of the system have a high magnitude, analogous case when the properties are small. Missoum et al, (2013) [2] obtained data for both methods, showing a great difference between them for not taking into account many variables in the analytical method, it is suggested to use a hot chamber with a guard in order to know which method is the more precise.

Before the construction of any experimental design, it is necessary to represent mathematics in order to have the necessary knowledge to assess the results obtained through experimental work and determine which are the most sensitive parameters to take into account.

The objective of this study is to represent the numerical and analytical design of a heat transfer process in one direction, under non-stationary conditions, through a wall with third-class boundary conditions on both sides of it.

This work is part of the design, construction and calibration of a Hot Chamber with Guard that is used to determine the heat and mass transfer coefficients in building walls in order to obtain the necessary information to carry out an adequate design of the buildings.

Description of the numerical method

Consider a wall isolated at its upper and lower ends, as shown in Figure 1. The other two faces of the wall are at different temperatures. The outside temperature varies sinusoidally and the temperature inside remains constant. The boundaries on both sides of the sample are convective and the remaining boundaries are adiabatic. The initial temperature distribution is uniform with the same value as the interior temperature.

The non-steady state heat transfer process is described by the differential equation:

$$\rho C \frac{\partial T}{\partial t} = \frac{\partial}{\partial x}\left(\lambda \frac{\partial T}{\partial x}\right) \quad (1)$$

The physical properties of the materials that make up the wall are described in Table 1.

Graphic 1 Wall configuration

Property	Magnitude
Thickness, cm	10
Thermal conductivity, W / (m ° C)	0.8
Specific heat, J / kg ° C	900
Density, kg / m³	1400

Table 1 Physical properties of masonry

ISSN 2531-2979

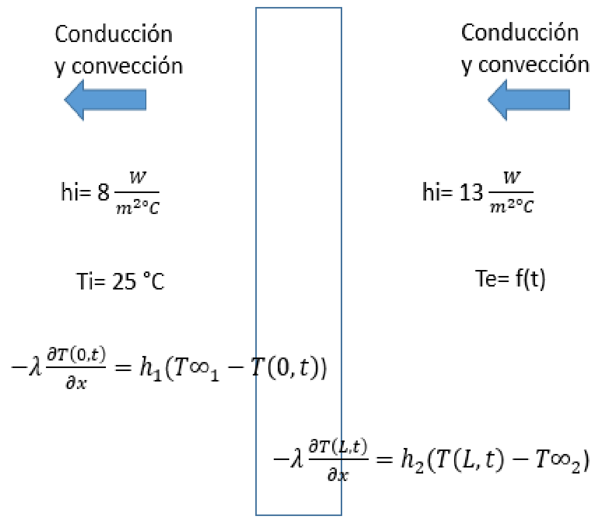

Graphic 2 Condiciones de frontera

The heat transfer is carried out in only one direction, horizontal; and under non-stationary regime. The boundary conditions that are presented are on both sides of Third Class or convection. In Figure 2 the boundary conditions on both sides of the wall are presented. For one-dimensional heat transfer in the x direction, in a plate of thickness L, the boundary conditions on both surfaces can be expressed as:

$$-\lambda \frac{\partial T(0,t)}{\partial x} = h_1\big(T\infty_1 - T(0,t)\big) \qquad (2)$$

$$-\lambda \frac{\partial T(L,t)}{\partial x} = h_2(T(L,t) - T\infty_2) \qquad (3)$$

Where: h is the convective coefficient operating on each exposed surface and T∞ is the ambient temperature on each side of the wall. For the internal side of the wall, the initial parameters shown in Table 2 are defined. While for the external side of the wall, the initial parameters are those shown in Table 3.

Propiedad	Magnitud
Coeficiente covectivo interno, W/m2 °C	8
Temperatura interna, °C	25

Table 2 Indoor temperature conditions

Propiedad	Magnitud
Coeficiente convectivo externo, W/m2 °C	13
Temperatura Externa, °C	Función del tiempo

Table 3 External temperature conditions

As the external temperature is dependent on time, there is a transient heat transfer process. The external temperature is defined by Equation (4), which defines the external ambient temperature for a period of 24 hours.

$$Tamb(t) = 28 + 15sen(\tfrac{2\pi t}{86400}) \qquad (4)$$

The finite element method (FEM) was used to solve the problem [3]. The FEM is a numerical method for solving differential equations, which is based on dividing the body, structure or domain (continuous medium) on which certain integral equations are defined that characterize the physical behavior of the problem, in a series of subdomains not intersecting with each other called finite elements. The set of finite elements forms a partition of the domain also called discretization. Within each element a series of representative points called nodes are distinguished. The set of nodes considering their adjacency relationships is known as a mesh. According to these adjacency or connectivity relationships, the value of a set of unknown variables defined at each node and called degrees of freedom is related.

The set of relationships between the value of a certain variable between the nodes can be written in the form of a system of linear equations, the matrix of said system of equations is called the stiffness matrix of the system. The number of equations in this system is proportional to the number of nodes.

The numerical solution of a differential heat transfer equation consists of fixing a number of points in the system from which temperature values will be obtained and a temperature distribution will be constructed. This temperature distribution must be defined by a discretiation of the physical domain in which the heat transfer takes place in subdomains that will form a mesh of interconnected nodes. A typical discretization of the domain is represented in Figure 3.

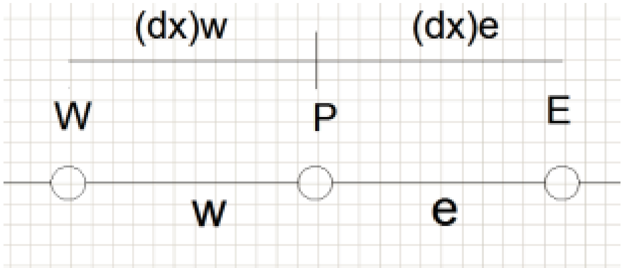

Graphic 3 Discretization of the physical environment

The discretization equations are listed below:

$$\frac{k_e(T_E-T_P)}{(\delta x)_e}-\frac{k_w(T_P-T_W)}{(\delta x)_w}+S\Delta x=0 \quad (5)$$

Equation (6) describes the physical phenomenon by means of the equilibrium equation.

$$\begin{aligned} a_pT_p = a_E[fT_E+(1-f)T^0{}_E] \\ + a_w[fT_W+(1-f)T^0{}_w] \\ + [a^0{}_p-(1-f)a_E \\ -(1-f)a_E] \end{aligned} \quad (7)$$

$$a_E=\frac{\lambda_e}{(\delta x)_e} \quad (8)$$

$$a_W=\frac{\lambda_w}{(\delta x)_w} \quad (9)$$

$$a^0{}_p=\rho C\frac{\Delta x}{\Delta t} \quad (10)$$

$$a_p=fa_E+fa_W+a^0{}_p \quad (11)$$

Weight factor

For certain values of the weight factor f, the discretization of the equation is reduced to a scheme of known equations, which are described below:

Explicit method (f = 0), it assumes that the values in the previous time instant prevail throughout the analysis time interval t + Δt.

Implicit method (f = 1), postulates that at time t, Tp passes from $TP\ a\ TP$ and subsequently remains at TP throughout the analysis interval, so that the new temperature value is characterized by $T1$

Crank-Nicholson method (f = 0.5), indicates a linear variation of Tp. At first glance, the linear variation would seem more sensitive than the other two schemes, considering leading and lagging values equally.

With the coefficients obtained with the equations described above, we proceed to construct a tridiagonal matrix, in which its main diagonal contains the values related to node P, the matrix below the diagonal contains the coefficients of node W and the diagonal above the main one. represents the coefficients of node E. In Equation (12) the resulting matrices and vectors for a 5-node mesh are shown.

The result vector contains the temperatures at each node of the mesh in the system. The multiplication of the matrix of coefficients by the vector of results gives as a result the vector of constants, for which the first value and the last one depend on the defined boundary conditions, for the case of third class conditions, the product is considered of the convective coefficient, the thermal conductivity, the length differential and the ambient temperature on that side of the border [4].

$$\begin{bmatrix} a_P & -a_E & 0 & 0 & 0 \\ -a_W & a_P & -a_E & 0 & 0 \\ 0 & -a_W & a_P & -a_E & 0 \\ 0 & 0 & -a_W & a_P & -a_E \\ 0 & 0 & 0 & -a_W & a_P \end{bmatrix} x \begin{Bmatrix} T_1 \\ T_2 \\ T_3 \\ T_4 \\ T_5 \end{Bmatrix} = \begin{Bmatrix} h_i \frac{\lambda_e}{dx_e} T_i \\ b \\ b \\ b \\ h_e \frac{\lambda w}{dx_w} T_e \end{Bmatrix} \quad (12)$$

Description of the analytical method

Considering the wall described in Graph 1, a mathematical model is proposed under the following considerations:

– The initial temperature distribution and the physical properties of the wall are homogeneous.

– The convective coefficients and the ambient temperature are uniform over the sample, that is, they do not depend on the position.

ISSN 2531-2979

– With the previous considerations the problem can be reduced to a one-dimensional model [5]. The governing equation that governs the phenomenon is as follows:

Governing equation

$$\frac{\partial^2 T(x,t)}{\partial x^2} = \frac{1}{\alpha}\frac{\partial T(x,t)}{\partial t} \quad \text{en } 0 < x < L,\ t > 0 \tag{13}$$

Boundary conditions:

Same boundary conditions as in the approach of the analytical method. See equations (2) and (3). Transient variation of the external ambient temperature:

$$T(t)_{ambiente} = T_{int} + T_c + T_a \sin(\omega t) \tag{14}$$

$\omega = \frac{2\pi}{86400}$ es la frecuencia angular diaria, T_{int} es la temperatura interior, T_c es la desviación entre el valor medio de la temperatura ambiente diaria y la temperatura interior y T_a es la amplitud de los cambios en la temperatura exterior.

Mathematical model solution

For the solution of the mathematical model, the following procedure is followed:

Step 1 a variable change is made to reduce the number of non-homogeneous borders as follows:

$$\frac{\partial^2 \Phi(x,t)}{\partial x^2} = \frac{1}{\alpha}\frac{\partial \Phi(x,t)}{\partial t} \quad \text{en } 0 < x < L,\ t > 0 \tag{15}$$

y las condiciones de frontera como

$$-\lambda\frac{\partial \Phi}{\partial x} + h_i\Phi = 0 \qquad \text{para } x = 0,\ t > 0 \tag{16}$$

$$\lambda\frac{\partial \Phi}{\partial x} + h_e\Phi = h_e\left(T(t)_{ambiente} - T_{int}\right) \qquad \text{para } x = L,\ t > 0 \tag{17}$$

donde $\left(T(t)_{ambiente} - T_{int}\right) = T_c + T_a \sin(\omega t)$

Step 2.- Solve for the auxiliary problem in transient state for a function with unit excitation.

$$\frac{\partial^2 \Phi(x,t)}{\partial x^2} = \frac{1}{\alpha}\frac{\partial \Phi(x,t)}{\partial t} \quad \text{en } 0 < x < L,\ t > 0 \tag{18}$$

y las condiciones de frontera como

$$-\lambda\frac{\partial \Phi}{\partial x} + h_i\Phi = 0 \qquad \text{para } x = 0,\ t > 0 \tag{19}$$

$$\lambda\frac{\partial \Phi}{\partial x} + h_e\Phi = 1 \qquad \text{para } x = L,\ t > 0 \tag{20}$$

La condición inicial es

$$\Phi(x,t) = f(x) - T_{int} \text{ para } 0 < x < L \tag{21}$$

la solución es $\Phi = \Phi_p + \Phi_t$

Φ_p solución de estado permanente

Φ_t solución transitoria.

Step 2.1- Solve the permanent part of the auxiliary problem

$$\frac{\partial^2 \Phi_p(x,t)}{\partial x^2} = 0 \qquad \text{en } 0 < x < L \tag{22}$$

y las condiciones de frontera como

$$-\lambda\frac{\partial \Phi_p}{\partial x} + h_i\Phi_p = 0 \qquad \text{para } x = 0,\ t > 0 \tag{23}$$

$$\lambda\frac{\partial \Phi_p}{\partial x} + h_e\Phi_p = 1 \qquad \text{para } x = L,\ t > 0 \tag{24}$$

Solución general

$$T = C_1 x + C_2 \tag{25}$$

ISSN 2531-2979

Solución particular

$$-\lambda\frac{\partial\Phi_p}{\partial x}+h_i\Phi_p=0; \qquad H_1=\frac{h_i}{\lambda};$$

$$-\frac{\partial\Phi_p}{\partial x}+H_1\Phi_p=0; \qquad -C_1+H_1\left(C_1x+C_2\right)=0$$

en $x=0$

$$-C_1+H_1C_2=0$$

$$\lambda\frac{\partial T}{\partial x}h_eT=1; \qquad H_2=\frac{h_e}{\lambda};$$

$$\frac{\partial T}{\partial x}+H_2T=\frac{1}{\lambda}; \qquad C_1+H_2\left(C_1x+C_2\right)=\frac{1}{\lambda}$$

en $x=L$

$$\left(H_2L+1\right)C_1+H_2C_2=\frac{1}{\lambda}$$

$$-C_1+H_1C_2=0$$

$$\left(H_2L+1\right)C_1+H_2C_2=\frac{1}{\lambda}$$

$$C_1=\frac{H_1}{\left(H_1H_2L+H_1+H_2\right)\lambda}$$

$$C_2=\frac{C_1}{H_1}$$

Step 2.2- Solution of the transitory part of the auxiliary problem.

$$\frac{\partial^2\Phi_t\left(x,t\right)}{\partial x^2}=\frac{1}{\alpha}\frac{\partial\Phi_t\left(x,t\right)}{\partial t} \quad \text{en } 0<x<L,\ t>0 \tag{26}$$

y las condiciones de frontera como

$$-\lambda\frac{\partial\Phi_t}{\partial x}+h_i\Phi_t=0 \qquad \text{para } x=0\,,t>0 \tag{27}$$

$$\lambda\frac{\partial\Phi}{\partial x}+h_e\Phi=0 \qquad \text{para } x=L\,,t>0 \tag{28}$$

La condición inicial es

$$\Phi_0\left(x,t=0\right)=F\left(x\right)-\Phi_p\left(x,t\right) \quad \text{para } 0<x<L \text{ y } t=0 \tag{29}$$

$$\Phi_t\left(x,t\right)=\sum_{m=1}^{\infty}e^{-\alpha\beta_m^2t}\frac{1}{N\left(\beta_m\right)}X\left(\beta_m,x\right)\ldots\int_0^L X\left(\beta_m,x'\right)\Phi_0\left(x',t=0\right)dx' \tag{30}$$

Donde se definen las expresiones:

$$\frac{1}{N\left(\beta_m\right)}=2\left[\beta_m^2+H_1^2\left(L+\frac{H_2}{\beta_m^2+H_2^2}\right)+H_1\right]^{-1} \tag{31}$$

$$X\left(\beta_m,x\right)=\beta_m\cos\left(\beta_mx\right)+H_1\sin\left(\beta_mx\right) \tag{32}$$

$$\tan\left(\beta_mL\right)=\frac{\beta_m\left(H_1+H_2\right)}{\beta_m^2-H_1H_2} \tag{33}$$

$$\Phi\left(x,t\right)=\Phi_p\left(x,t\right)+\Phi_t\left(x,t\right) \tag{34}$$

$$\Phi\left(x,t\right)=C_1x+C_2+T_{int}+\sum_{m=1}^{\infty}e^{-\alpha\beta_m^2t}\frac{1}{N\left(\beta_m\right)}X\left(\beta_m,x\right)\ldots\int_0^L X\left(\beta_m,x'\right)\Phi_0\left(x',t=0\right)dx' \tag{35}$$

reemplazando t por $t-\tau$

$$\Phi\left(x,t-\tau\right)=T_{int}+C_1x+C_2+\sum_{m=1}^{\infty}e^{-\alpha\beta_m^2(t-\tau)}2\left[\beta_m^2+H_1^2\left(L+\frac{H_2}{\beta_m^2+H_2^2}\right)+H_1\right]^{-1}\ldots\left(\beta_m\cos\left(\beta_mx\right)+H_1\sin\left(\beta_mx\right)\right)\ldots\int_0^L\left(\beta_m\cos\left(\beta_mx\right)+H_1\sin\left(\beta_mx\right)\right)\Phi_0\left(x',t=0\right)dx' \tag{36}$$

$$T\left(x,t\right)=\int_{\tau=0}^{t}\Phi\left(x,t-\tau\right)\frac{df\left(\tau\right)}{d\tau}d\tau \qquad para\ t\prec\tau_1 \tag{37}$$

$$\frac{\partial T}{\partial x}+H_2T=\underbrace{H_2\left(T_a\sin\left(\omega t\right)\right)}_{f(\tau)} \qquad \text{para } x=L,t>0 \tag{38}$$

$$\frac{df\left(H_2\left(T_a\sin\left(\omega\tau\right)\right)\right)}{d\tau}=H_2T_a\omega\cos\left(\omega\tau\right) \tag{39}$$

ISSN 2531-2979

Step 3. Applying Duhamel's theorem the solution obtained has the form:

$$T(x,t)=T_{int}+Tp+h_cT_a\sum_{m=1}^{\infty}\frac{-\alpha\beta_m^{2}\omega e^{-\alpha\beta_m^{2}t}+\alpha\beta_m^{2}\omega\cos\omega t-\alpha^{2}\beta_m^{4}\sin\omega t}{\left(\alpha^{2}\beta_m^{4}+\omega^{2}\right)N\left(\beta_m\right)}\ldots$$

$$X\left(\beta_m x\right)\int_0^L-\left(C_1x+C_2\right)\left(X\left(\beta_m x\right)\right)dx \qquad (40)$$

Results

Due to the large number of results obtained, an average of the temperatures between the three numerical calculation schemes and the average difference between the numerical and analytical methods have been obtained at the three points of interest of the masonry wall. Graph 4 shows the 48-hour process for the explicit numerical scheme, establishing a time step of 1 second and 7 analysis nodes. While in Graph 5 the comparison of the three calculation schemes for a small interval is represented, where it is shown that there are no significant variations and it could be considered that for this case study the three schemes provide the same results.

On the other hand, the results obtained through the analytical simulation are presented in Graph 6.

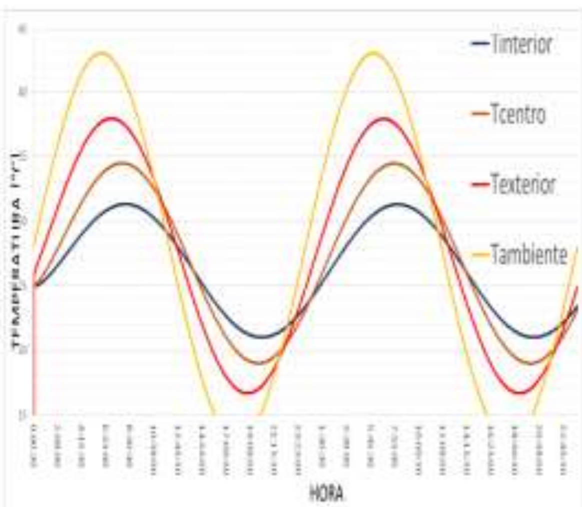

Graphic 4 Result

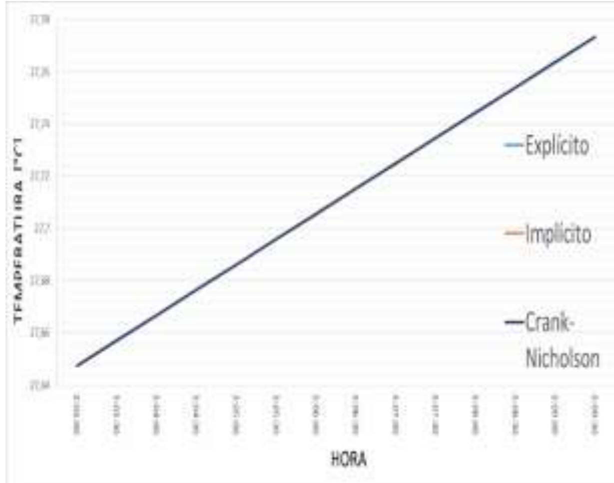

Graphic 5 Result for dt = 30 and 7 nodes

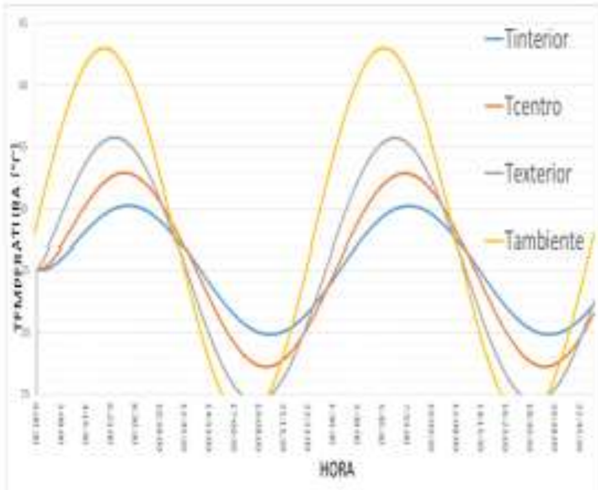

Graphic 6 Analytical method results

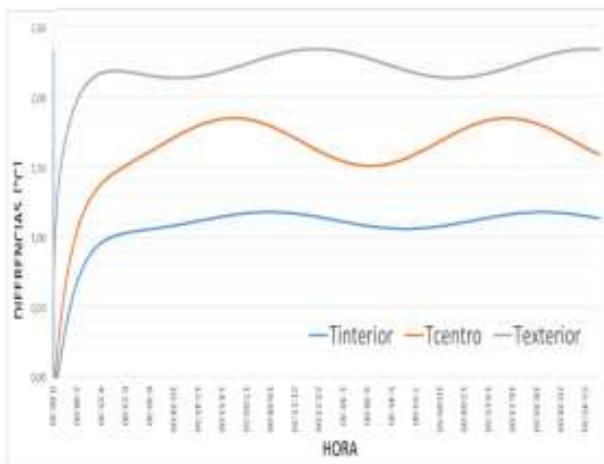

Graphic 7 Differences between analytical and numerical method

Graph 6 shows the differences between the average temperatures of the three numerical schemes compared to the analytical method. As shown, the temperatures tend to vary in the first moments of the analysis to later take on relatively stable behaviors.

Both methods converged to a very approximate solution to each other, with absolute values of difference of only 2.34 ° C, which for the calculation purposes that are intended to be carried out is considered a tolerable uncertainty.

Table 4 summarizes the differences obtained between the averages of the temperatures obtained at the internal, central and external points with respect to the results obtained in the analytical method. In this case, the results obtained for the 1 second time step are presented with the quantities of discretization nodes of the medium of 7, 11, 15, 19 and 23 nodes.

In this study, the passage of time and the number of nodes of the discretization of the medium did not play a transcendental role to mark strong differences in results. This is due to the fact that in only 2 simulations the equality required by the explicit scheme to be able to calculate temperatures was not fulfilled, while in the rest of the simulations, the value that relates the passage of time and space was found very far from the critical value.

	Diferencias promedio en %		
Simulación	T(Interior)	T(Centro)	T(Exterior)
Dt=1 ... Nx=7	-4,38%	-6,85%	-9,72%
Dt=1 ... Nx=11	-4,44%	-6,94%	-9,82%
Dt=1 ... Nx=15	-4,46%	-6,98%	-9,87%
Dt=1 ... Nx=19	-4,48%	-7,00%	-9,89%
Dt=1 ... Nx=23	-4,49%	-7,02%	-9,91%
Promedio	-4,45%	-6,96%	-9,84%

Tabla 4 Diferencias en porcentaje para Dt=1 [s] y Nx= 23 nodos.

	Desviaciones estándares		
Simulación	T(Interior)	T(Centro)	T(Exterior)
Dt=1...Nx=7	1,15%	2,25%	3,50%
Dt=1...Nx=11	1,45%	2,62%	3,78%
Dt=1...Nx=15	1,61%	2,80%	3,92%
Dt=1...Nx=19	1,71%	2,91%	4,01%
Dt=1...Nx=23	1,78%	2,98%	4,06%
Promedio	1,54%	2,71%	3,85%

Tabla 5 Desviaciones estándares en los porcentajes e diferencia.

Table 5 shows the standard deviations of the mean differences between the schemes of the numerical method and the analytical method

Acknowledgments

We are grateful to CONACYT for the financing granted for the development of this project, and to the Universidad Juárez Autónoma de Tabasco for the facilities to carry it out.

Conclusions

The results obtained through the numerical simulation in the three schemes for the same magnitudes of time passage and number of nodes differ insignificantly from each other, variations of the order of 0.003% were quantified. Therefore, it is concluded that the three calculation schemes provide practically the same results.

On the other hand, the differences between analytical and numerical methods were quantified with average values in the interior point of 4.45%, in the central point of 6.96% and in the external node of 9.84%. The notable differences in temperature variations between the analyzed nodes are attributed to the fact that in the external node, which is where a transient external temperature operates, there are higher maximum and minimum temperature ranges.

Therefore, these results are more likely to vary strongly, which is confirmed by the standard deviation of 3.85% calculated at this point, while in the internal node it was only 1.54%.

References

[1] Sushas V. Patankar . (1980). Numerical Heat Transfer and Fluid Flow. Minesota: Hemisphere Publishing Coorporation.

[2] A Missoum. (2013). Numerical Simulation of Heat Transfer through a Double-walled Facade Building in Arid Zone . Energy Procedia, 36, 834-843.

[3] Sushas V. Patankar . (1980). Numerical Heat Transfer and Fluid Flow. Minesota: Hemisphere Publishing Coorporation.

[4] David Incropera. (2011). Fundamentals of Heat and Mass Transfer. New Jersey: John Wiley & Sons.

[5] David W. Hahn. (2012). Heat Conduction. John Wiley & Sons: New Jersey.